Available online at www.sciencedirect.com
SCIENCE DIRECT®
Journal of Magnetic Resonance 171 (2004) 305–313
JMR Journal of Magnetic Resonance
www.elsevier.com/locate/jmr

Exact half pulse synthesis via the inverse scattering transform

Jeremy Magland, Charles L. Epstein*,[1]

LSNI, Department of Radiology, HUP, University of Pennsylvania, United States
Department of Mathematics, University of Pennsylvania, United States

Received 7 January 2004; revised 9 September 2004
Available online 8 October 2004

Abstract

In a paper of Nielson et al. it is shown, using the linear approximation, that it might be possible to create a pair of RF-pulses, which, after summation of the unrephased signals achieve a specified transverse magnetization. Such pulses, designed using the linear approximation, show rather poor slice selectivity. Using the inverse scattering transform formalism we give an algorithm to exactly achieve a specified "summed" transverse magnetization profile. Indeed for a constant phase transverse profile, our algorithm produces infinitely many solutions.

Keywords: Nuclear magnetic resonance; Imaging; RF-pulse synthesis; Selective excitation; Inverse scattering; Half pulse; Rephasing

1. Introduction

When imaging very short T_2 species, it is useful to be able to begin acquiring a signal as soon as possible after the RF-excitation. In particular, one would like to reduce the length of the excitation and rephasing time, essentially to 0. The possibility of using two "half pulses" is explored by Nielson et al. in [4]. They consider the following question: suppose we are given a target transverse magnetization profile $(m_x^s + \mathrm{i}m_y^s)(f)$, here f is the offset frequency. Can we find a pair of self refocused, pulses $q_1(t)$ and $q_2(t)$ with magnetization profiles, $(m_x^1 + \mathrm{i}m_y^1)(f)$, $(m_x^2 + \mathrm{i}m_y^2)(f)$, so that

$$(m_x^s + \mathrm{i}m_y^s)(f) = \left[(m_x^1 + \mathrm{i}m_y^1)(f) + (m_x^2 + \mathrm{i}m_y^2)(-f)\right]? \tag{1}$$

By "self refocused" we mean that, at the conclusion of the RF-pulse, the magnetizations achieve the stated transverse profiles, in this case $(m_x^1 + \mathrm{i}m_y^1)(f)$ and $(m_x^2 + \mathrm{i}m_y^2)(f)$, respectively, without any need for rephasing. We call the pair, $(q_1(t), q_2(t))$, a pair of *half pulses*. In this paper we normalize so that the magnetization profile, $\mathbf{m}(f) = [m_x(f), m_y(f), m_z(f)]$, produced by a *single* pulse, is a $\mathbb{R}^3$ valued function of length 1. The intuition behind the usage of half pulses, which mostly comes from the linear theory, is very well explained in the Nielson et al. paper.

The intent of this paper is to present an exact solution to the design problem. This is the essentially mathematical question of finding the half pulse pairs whose transverse profiles satisfy Eq. (1). We accomplish this by rephrasing the half pulse design as an inverse scattering problem. Using the formalism introduced in [2], this inverse scattering problem is solved.

A reason to use half pulses is that they can considerably shorten the excitation part of a pulse sequence, without sacrificing selectivity or increasing the bandwidth. They are especially useful when imaging objects, such as bone, which have a very short T_2, see, for example, Gatehouse and co-workers [7]. There are two reasons for this: (1) They do not require rephasing. (2) A typical half pulse has a single large peak at the end, and there is little transverse magnetization (which is

* Corresponding author.
E-mail address: cle@math.upenn.edu (C.L. Epstein).
[1] Research of both authors was partially supported by NSF Grant DMS02-03705.

1090-7807/$ - see front matter © 2004 Elsevier Inc. All rights reserved.
doi:10.1016/j.jmr.2004.09.004

subject to T_2-relaxation) before this peak. For example, each pulse in a reasonably selective 2 kHz half pulse pair has a duration of about 2.5 ms. The comparable minimum energy pulse has a duration of about 5 ms and requires about 2.5 ms of rephasing. Comparing Figs. 1–3C to Fig. 4C, where the pulses are played out with $T_2 = 5$ ms, we see that the profile produced by a minimum energy pulse looses more than half its amplitude whereas, the profiles produced by the half pulses are almost unaffected. Several other applications of half pulses are described in Nielson et al., for example, in MR angiography.

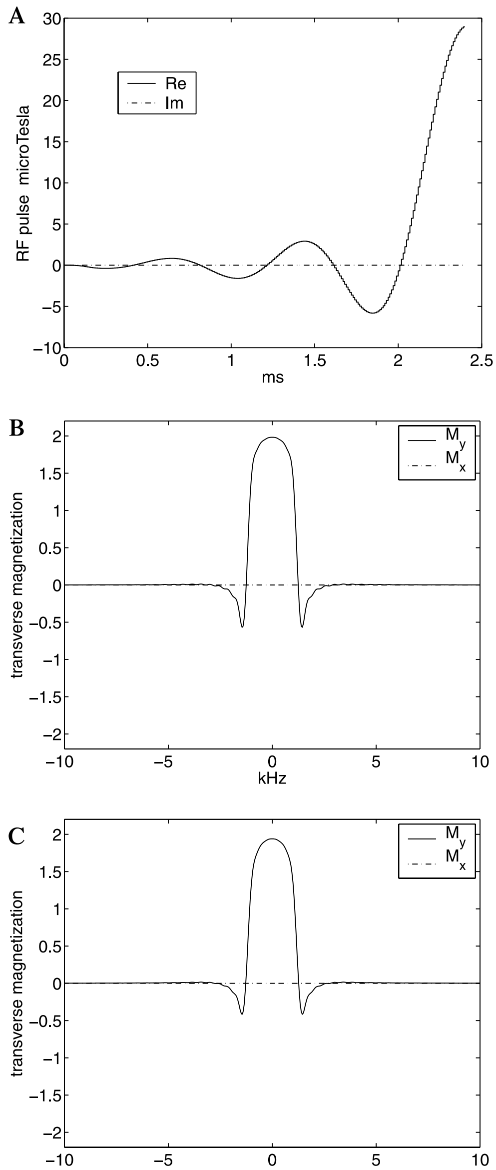

Fig. 1. The result of using the linear approximation to design a pair of half pulses which sum to produce the maximum possible in-slice signal. (A) Pulse designed using the linear approximation. (B) The summed transverse magnetization produced by using the pulse in (A) as a half pulse, with $T_2 = \infty$. (C) The summed transverse magnetization produced by using the pulse in (A) as a half pulse, with $T_2 = 5$ ms.

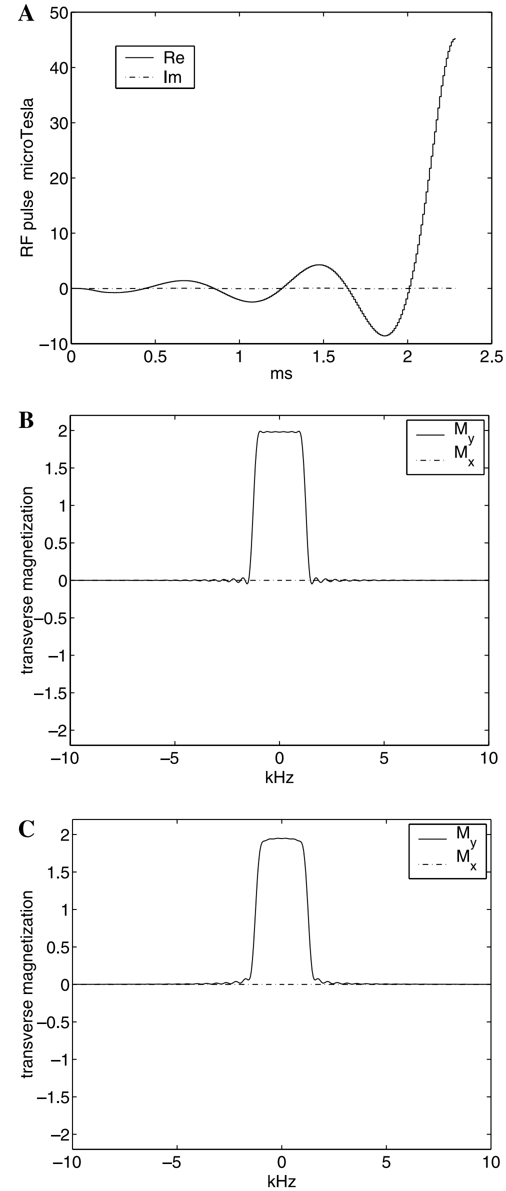

Fig. 2. This shows the nonlinear half pulse used to obtain a maximum summed profile. (A) An IST half pulse. (B) The summed transverse magnetization produced by using the pulse in (A) with $T_2 = \infty$. (C) The summed transverse magnetization produced by using the pulse in (A) with $T_2 = 5$ ms.

Due to the nonlinear dependence of the magnetization profile on the pulse envelope, the problem of finding a half pulse pair, $(q_1(t), q_2(t))$, given $(m_x^s + \mathrm{i}m_y^s)(f)$ is clearly nonlinear. The Nielson paper solves this problem to first order, using the low flip angle connection between the Fourier transform of the pulse envelope, and the transverse magnetization profile, see [6]. In the natural time parameterization provided by the inverse scattering formalism, a pulse is self refocused if it is supported in $(-\infty, 0]$, see [2,8]. In this time parameterization, the Fourier transforms of $q_1(t)$ and $q_2(t)$ would therefore have analytic continuations to the upper half

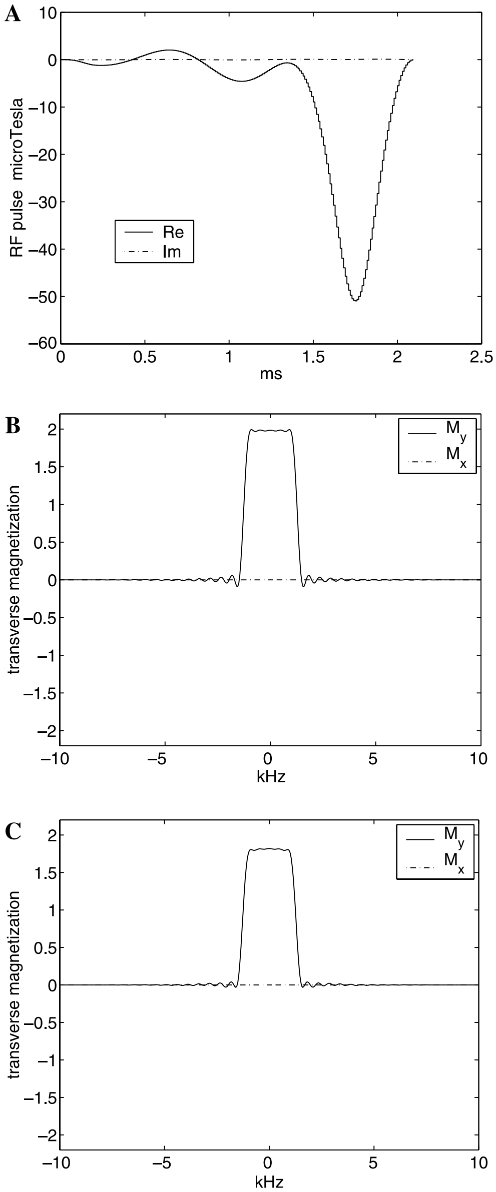

Fig. 3. This shows the nonlinear half pulse used to obtain a maximum summed profile with a Blaschke factor included to reduce the out-of-slice imaginary part. (A) The half pulse. (B) The summed transverse magnetization produced by using the pulse in (A) with $T_2 = \infty$. (C) The summed transverse magnetization produced by using the pulse in (A) with $T_2 = 5$ ms.

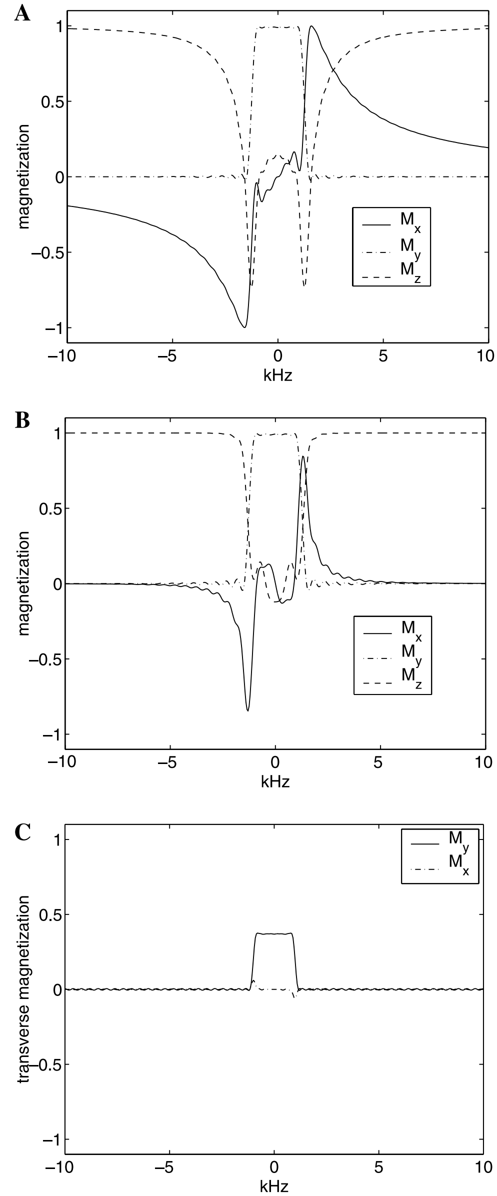

Fig. 4. Plots (A and B) show the (unsummed) magnetization profiles produced by two pulses designed using the IST method. (A) The magnetization profile produced by the pulse in Fig. 2A. (B) The magnetization profile produced by the pulse in Fig. 3A. (C) The transverse magnetization produced by a minimum energy IST pulse, with a rephasing time of 2.5 ms, and $T_2 = 5$ ms. If $T_2 = \infty$ the in-slice transverse magnetization produced by this pulse has size 1. This plot should be compared to Figs. 1–3C.

plane. The mathematical content of the Nielson paper is contained in the following classical theorem:

Theorem 1. *Let* $g(f) \in L^2(\mathbb{R})$, *then there are unique functions* $g_1(f)$, $g_2(f)$ *in* $L^2(\mathbb{R})$ *such that* $g_1(f)$ *and* $g_2(f)$ *have analytic extensions to the upper half plane and* $g(f) = g_1(f) + g_2(-f)$.

In the next section we rephrase the problem of finding pairs of half pulses in the inverse scattering formalism presented in [2]. We first give a simple closed form solution, provided the target magnetization is real. This is the case of principal interest in applications. Like other pulse synthesis problems, this problem has an infinite dimensional space of solutions, which we produce. We then give an algorithm to find the unique small energy solution for sufficiently small, complex valued data. In practice we have found that this algorithm works well, even for fairly large data. The case of a nonreal summed transverse profile is analyzed in Appendix B. In the final section we give the half pulse pairs for several target magnetizations.

2. Half pulse synthesis as an inverse scattering problem

A pair of half pulses would be used in an MR-experiment as follows (we assume here the possibility of instantaneously switching the gradient fields): with the slice select gradient turned on, the sample is first excited using the profile $q_1(t)$. At the conclusion of the excitation, the slice select gradient is immediately turned off, and the signal $S_1(t)$ is acquired. Once the system has returned to equilibrium, the slice select gradient is again turned on, *but with the polarity reversed*. The sample is excited using the profile $q_2(t)$. At the conclusion of this excitation the slice select gradient is again, immediately turned off, and the signal $S_2(t)$ is acquired. The goal of half pulse design is to have the summed signal, $S(t) = S_1(t) + S_2(t)$, equal to the signal that would have resulted if we had used a selective pulse with transverse profile $(m_x^s + \mathrm{i}m_y^s)(f)$.

In fact we can do even better than we could have done with a single excitation. With our normalization, the transverse profile produced by a single pulse is restricted to have norm less than 1. Because it is the result of summing the signals from two such excitations, the norm of the summed profile (in Eq. (1)) may be arbitrarily close to 2. For this reason we restrict the target summed profile, $(m_x^s + \mathrm{i}m_y^s)(f)$, to be a function taking values in the disk of radius 2, rather than the disk of radius 1, as would be the case for the design of a single pulse. Using the half pulse technique one can also increase the SNR by $\sqrt{2}$: the *summed* signal has double the usual amplitude, while the noise is uncorrelated between the two half pulse excitations. Beyond this increase in SNR, the individual pulses $q_1(t)$ and $q_2(t)$ have large effective bandwidths and this tends to decrease their durations. This is a great virtue when imaging species with very short spin–spin relaxation rates. In light of the linearity of the measurement process, it is also clear that one can follow the excitations with phase, or frequency encoding steps, and the statement about the sum of the measured signals remains correct. Another way to achieve excitations that require no rephasing time is to use bound states to obtain self refocused 90° pulses, see [3,8]. For a given bandwidth (in the summed profile), the standard self refocused pulses are considerably longer than the half pulses we design here and have much larger maximum amplitudes.

In [2], a formalism is presented for analyzing pulse synthesis problems using the inverse scattering transform (IST). We only require a few facts, which we now present. Given a magnetization profile, which is a unit 3-vector valued function,

$$\mathbf{m}^{\infty}(\xi) = [m_x^{\infty}(\xi), m_y^{\infty}(\xi), m_z^{\infty}(\xi)],$$

the IST algorithm finds a pulse envelope $q(t)$, which, after appropriate rephasing, produces the given profile. The parameter $\xi = \frac{f}{2}$ is the natural spin domain offset frequency parameter. The pulse synthesis problem is highly underdetermined, and the IST actually allows one to specify an arbitrary number of auxiliary parameters. For the moment, we restrict our attention to minimum energy pulses, which are uniquely determined by the magnetization profile. A detailed discussion of IST pulse synthesis can be found in [2]. We use the results of that paper freely.

In the inverse scattering formalism, the natural datum for specifying the frequency response is the reflection coefficient, $r(\xi)$. If, in the natural time parametrization provided by the inverse scattering transform, the pulse is supported in the interval $(-\infty, t_1]$, then the reflection coefficient is related to the magnetization profile by

$$r(\xi) = \frac{(m_x^{\infty}(\xi) + \mathrm{i}m_y^{\infty}(\xi))\mathrm{e}^{-2\mathrm{i}\xi t_1}}{1 + m_z^{\infty}(\xi)}. \tag{2}$$

As noted above, the magnetization profile, $\mathbf{m}^{\infty}(\xi)$, produced by a *single* pulse is a unit vector valued function. In applications to MR, the transverse component is usually supported in a bounded interval.

Supposing the gradient polarity is simply reversed, Eq. (2) implies that a pulse supported in $(-\infty, t_1]$ requires t_1 units of rephasing time to achieve the *specified* magnetization profile, i.e, $\mathbf{m}^{\infty}(\xi)$. This explains our remark, that a pulse supported in $(-\infty, 0]$ is a self refocused pulse: it attains the specified magnetization profile without any need for rephasing. Using Eq. (2), with $t_1 = 0$, we obtain the formula

$$m_x^{\infty}(\xi) + \mathrm{i}m_y^{\infty}(\xi) = \frac{2r(\xi)}{1 + |r(\xi)|^2}. \tag{3}$$

To simplify, the notation we set $\mathbf{m}_{xy}(\xi) = m_x(\xi) + \mathrm{i}m_y(\xi)$. With our normalization, the transverse magnetization profile $\mathbf{m}_{xy}^{\infty}(\xi)$, produced by a single pulse, is a complex valued function, defined on the real line, taking values in the unit disk.

A minimum energy pulse is supported in $(-\infty, 0]$ if and only if its reflection coefficient $r(\xi)$ has an analytic extension to the upper half plane. More generally, a pulse is supported in $(-\infty, 0]$ if $r(\xi)$ has a meromorphic extension to the upper half plane, with finitely poles, and these poles of $r(\xi)$ are used to define the bound states. We give a short proof of this statement in Appendix A. With these preliminaries we can now recast the half pulse synthesis problem in terms of scattering data: given a summed transverse magnetization profile $\mathbf{m}_{xy}^s(\xi)$, find a pair of reflection coefficients $(r_1(\xi), r_2(\xi))$ such that:

1. $r_1(\xi)$ and $r_2(\xi)$ have analytic extensions to the upper half plane, or meromorphic extensions with finitely many poles.
2. For $\xi \in \mathbb{R}$, they satisfy the equation:

$$\frac{2r_1(\xi)}{1 + |r_1(\xi)|^2} + \frac{2r_2(-\xi)}{1 + |r_2(-\xi)|^2} = \mathbf{m}_{xy}^s(\xi). \tag{4}$$

We emphasize that, for the half pulse problem, the input datum is a summed transverse profile $\mathbf{m}_{xy}^{s}(\xi)$, which is a complex valued function defined on the real line taking values in the disk of radius 2 centered at 0. The disk has radius 2 because $\mathbf{m}_{xy}^{s}(\xi)$ is the result of summing two transverse profiles, each of which takes values in the disk of radius 1. If $|\mathbf{m}_{xy}^{s}(\xi)|$ exceeds 1 at any point, then the given transverse magnetization can no longer be attained using a single pulse.

If $r_1(\xi)$ and $r_2(\xi)$ have analytic extensions, then the corresponding minimum energy pulses $q_1(t)$, $q_2(t)$, with these reflection coefficients are supported in $(-\infty, 0]$, and therefore solve the half pulse synthesis problem. If $r_1(\xi)$, $r_2(\xi)$ are meromorphic with nontrivial poles, then we need to use the poles of $r_1(\xi)$ and $r_2(\xi)$, respectively, to define bound states, to get potentials, supported in $(-\infty, 0]$, with these reflection coefficients.

An interesting special case arises when $\mathbf{m}_{xy}^{s}(\xi)$ is real valued. In this case there is, in essence, a single half pulse that solves the problem. That is, $q_1(t)$ can be taken to be the pulse defined by $r_1(\xi)$ (and its poles in the upper half plane, if necessary). We then take $r_2(\xi) = r_1(-\xi^*)^*$. In this case Eq. (4) becomes:

$$\frac{4\mathrm{Re}\, r_1(\xi)}{1 + |r_1(\xi)|^2} = \mathbf{m}_{xy}^{s}(\xi). \tag{5}$$

Even when the datum, $\mathbf{m}_{xy}^{s}(\xi)$, is real, the solutions to Eq. (5) are not. The phase of $r_1(\xi)$ is fairly complicated, see Figs. 4A and B, and so it is necessary to use a method for obtaining the potential that respects the phase of the magnetization profile. In particular the usual Shinnar–Le Roux or SLR-approach cannot easily be applied. In the usual implementations of SLR, the pulse is designed using the flip angle profile and the phase is "recovered," see [5] or [2]. The half pulse synthesis problem is therefore a problem for which the IST approach to pulse synthesis is necessary. An exposition of a practical algorithm for implementing the IST-approach, with arbitrary bound states, is given in [3].

3. The solution in the real case

If $\mathbf{m}_{xy}^{s}(\xi)$ is real valued, then the half pulse design problem can be solved in closed form. Indeed the explicit formula provides an infinite dimensional space of solutions. These solutions have a simple formula in terms of the orthogonal projection Π_+ onto L^2 functions with an analytic extension to the upper half plane. This operator is defined in terms of the Fourier transform by

$$\Pi_+ f(\xi) = \frac{1}{2\pi}\int_0^{\infty} \hat{f}(t)\,\mathrm{e}^{\mathrm{i}t\xi}\,\mathrm{d}\xi = \frac{1}{2}(f + \mathcal{H}f). \tag{6}$$

Here $\mathcal{H}$ is the Hilbert transform. As $\mathcal{H}$ is a shift invariant filter, it can be efficiently implemented using the fast Fourier transform.

If we set

$$r_1(\xi) = \frac{1 - s(\xi)}{1 + s(\xi)}, \tag{7}$$

then Eq. (5) becomes

$$\frac{1 - |s(\xi)|^2}{1 + |s(\xi)|^2} = \tfrac{1}{2}\mathbf{m}_{xy}^{s}(\xi). \tag{8}$$

There exists a solution $s(\xi)$, to Eq. (8) that has a nonvanishing analytic extension to the upper half plane. Denote this solution by $s_0(\xi)$. Solving for $|s_0(\xi)|$, we obtain

$$|s_0(\xi)|^2 = \frac{2 - \mathbf{m}_{xy}^{s}(\xi)}{2 + \mathbf{m}_{xy}^{s}(\xi)}. \tag{9}$$

Given that $s_0(\xi)$ is analytic and nonvanishing in the upper half plane and tends to 1 as $|\xi|$ tends to infinity, we can use a knowledge of $|s_0(\xi)|$ to completely determine $s_0(\xi)$. This idea is already used in an essential way in the derivation of the IST, see Eqs. (38) and (40) in [2]. We use the projector Π_+ to solve for $\log s_0$ in terms of $\log|s_0|$. If we set

$$\begin{aligned}\log s_0(\xi) &= [\Pi_+ \log|s_0|](\xi) \\ &= \frac{1}{2}\Pi_+ \log\left[\frac{2 - \mathbf{m}_{xy}^{s}}{2 + \mathbf{m}_{xy}^{s}}\right](\xi),\end{aligned} \tag{10}$$

then

$$s_0(\xi) = \exp\left[\frac{1}{2}\Pi_+ \log\left[\frac{2 - \mathbf{m}_{xy}^{s}}{2 + \mathbf{m}_{xy}^{s}}\right](\xi)\right] \tag{11}$$

is a nonvanishing analytic function in the upper half plane, which satisfies Eq. (8) on the real axis. If $\mathbf{m}_{xy}^{s}(\xi)$ is integrable and has an integrable derivative, then $s_0(\xi)$ tends to 1 as $|\xi|$ tends to infinity.

Using Eqs. (7) and (10), we can easily solve for $r_1(\xi)$ in terms of $\mathbf{m}_{xy}^{s}(\xi)$. This function is meromorphic in the upper half plane, tends to zero at infinity, and satisfies Eq. (5). If $s(\xi) \neq -1$ for ξ in the upper half plane then $r_1(\xi)$ is analytic. This happens if, for example, $\mathbf{m}_{xy}^{s}(\xi)$ is nonnegative, then $|s_0(\xi)| \leqslant 1$ on the real axis, and so by the maximum principle, $s_0(\xi) \neq -1$ in the upper half plane.

We obtain the other solutions to Eq. (8) by multiplying $s_0(\xi)$ by a Blaschke product. Let $\boldsymbol{\zeta} = \{\zeta_1, \ldots, \zeta_N\}$ be an *arbitrary* collection of points with $\mathrm{Im}\zeta_j \neq 0$ for all j. The function defined by

$$s_{\zeta}(\xi) = s_0(\xi)\prod_{j=1}^{N}\left(\frac{\xi - \zeta_j}{\xi - \bar{\zeta}_j}\right) \tag{12}$$

satisfies Eq. (8) on the real axis and tends to 1 as $|\xi|$ tends to infinity in the closed upper half plane.

The functions $s_0(\xi)$ and $s_\zeta(\xi)$ are meromorphic in the upper half plane. Using formula (7) we recover $r_1(\xi)$ from $s_0(\xi)$, or $s_\zeta(\xi)$. The reflection coefficient is also meromorphic in the upper half plane. If $r_1(\xi)$ has poles, then these poles must be included as bound states when the potential $q_1(t)$ is reconstructed from $r_1(\xi)$. This is necessary to ensure that $q_1(t)$ is supported in $(-\infty,0]$. This provides a further reason why the IST approach to pulse synthesis is needed to reconstruct the potential from the scattering data. It is not immediately evident which, of the infinite dimensional space of possible half pulses, has the minimum energy.

We close this section by giving a useful application of the Blaschke factor. Since $s_0(\xi)$ is asymptotically equal to 1, the transverse magnetization $\frac{2r_1(\xi)}{1+|r_1(\xi)|^2}$ excited by the half pulse tends to zero as $|\xi|$ tends to infinity. However, the imaginary part of this function may decay very slowly (see Fig. 4A), which is undesirable in many applications. A method for improving the rate of decay is to choose $\boldsymbol{\zeta} = \{i\eta\}$, where $\eta \in \mathbb{R}$, is chosen so that

$$\lim_{|\xi|\to\infty} |\xi||s_\zeta(\xi) - 1| = 0. \tag{13}$$

This method is illustrated in Example 3.

4. The solution with general data

If $\mathbf{m}^s_{xy}(\xi)$ is not real valued, then there are many possible algorithms for obtaining approximations to $(r_1(\xi), r_2(\xi))$ and thereby $(q_1(t), q_2(t))$. In Appendix B we show that there is a unique low energy solution, if $\mathbf{m}^s_{xy}(\xi)$ is small enough. Here we give an algorithm that has successfully produced pulses, even for fairly large $\mathbf{m}^s_{xy}(\xi)$, i.e., functions with sup-norm close to 2. The algorithm we use is described in terms of the orthogonal projection Π_+, defined in Eq. (6).

The two reflection coefficients must be found simultaneously. We use the linear solution to initialize the algorithm:

$$r_1^0(\xi) = \tfrac{1}{2}\Pi_+[\mathbf{m}^s_{xy}(\xi)], \quad r_2^0(\xi) = \tfrac{1}{2}\Pi_+[\mathbf{m}^s_{xy}(-\xi)]. \tag{14}$$

The iteration is given by:

$$\begin{aligned} r_1^{j+1}(\xi) &= \Pi_+\left[\frac{(1+|r_1^j(\xi)|^2)}{2}\left(\mathbf{m}^s_{xy}(\xi) - \frac{2r_2^j(-\xi)}{1+|r_2^j(-\xi)|^2}\right)\right] \\ r_2^{j+1}(\xi) &= \Pi_+\left[\frac{(1+|r_2^j(\xi)|^2)}{2}\left(\mathbf{m}^s_{xy}(-\xi) - \frac{2r_1^j(-\xi)}{1+|r_1^j(-\xi)|^2}\right)\right]. \end{aligned} \tag{15}$$

The iterative step is repeated until the changes

$$\Delta r_1^{j+1}(\xi) = r_1^{j+1}(\xi) - r_1^j(\xi), \quad \Delta r_2^{j+1}(\xi) = r_2^{j+1}(\xi) - r_2^j(\xi)$$

become sufficiently small. It seems very likely that there is also an infinite dimensional space of solutions when $\mathbf{m}^s_{xy}$ is complex valued, though we have, as yet, no way to find the other solutions. In the next section we give an example of a half pulse pair designed using these algorithms.

5. Examples

In this section we give several examples, using the algorithms in Eqs. (10) and (15) to design pairs of half pulses. These equations are discretized and the solutions r_1, r_2 are found as finite Fourier series in $w = \exp(2i\Delta\xi)$. In effect we use a hard pulse approximation. The potentials, $q_1(t)$, $q_2(t)$ are obtained from the reflection coefficients, $r_1(w)$, $r_2(w)$, using a modification of an algorithm given by Yagle, see [9]. The input to this algorithm is a reflection coefficient r, which is a rational function of w. It automatically uses all the poles of r within the unit disk to define bound states, without the necessity to locate them or compute the residues of r at these points. Each of these pulses took considerably less than a minute to compute on a 2 GHz Linux box, using a Matlab program.

In the transverse profile plots, $m_x(f)$ is shown with a solid line and $m_y(f)$ is shown with a dot-dash line. The pulse plots are in the rotating reference frame. If $B_1(t) = e^{i\omega_0 t}(b_{1x}(t) + ib_{1y}(t))$ then, in the plots, $b_{1x}(t)$ is shown as a solid line and $b_{1y}(t)$ as a dot-dash line.

Example 1. Fig. 1A shows a half pulse designed using the Fourier method to produce a summed transverse profile equal to 2 within the passband and 0 a little outside it. In Fig. 1B we show the summed transverse profile produced by this pulse under "ideal" circumstances, i.e., $T_2 = \infty$. In Fig. 1C we show the summed transverse profile produced by this pulse with $T_2 = 5$ ms. Under ideal conditions this pulse is not very selective and fails to achieve the maximum summed amplitude within most of the passband. Even with a short T_2, the transverse profile retains most of its amplitude and shape.

Example 2. The pulse in Fig. 2A is designed with the IST algorithm and Eq. (10) to produce the summed transverse magnetization in-slice of 2 and essentially 0 out-of-slice. In Fig. 2B we show the summed transverse profile produced by this pulse under "ideal" circumstances, i.e., $T_2 = \infty$. In Fig. 2C we show the summed transverse profile produced by this pulse with $T_2 = 5$ ms. This pulse has somewhat larger maximum amplitude and equal duration to the previous example. Under ideal conditions it is very selective and produces essentially the full amplitude in-slice. With a short T_2, the transverse profile again retains most of its amplitude and selectivity.

Example 3. In this example we design a pulse with the same summed profile as in the previous example, using a Blaschke factor as described in Eq. (13). Fig. 3A shows the pulse. In Fig. 3B we show the summed transverse profile produced by this pulse under "ideal" circumstances, i.e., $T_2 = \infty$. In Fig. 3C we show the summed transverse profile produced by this pulse with $T_2 = 5$ ms. This pulse has somewhat larger maximum amplitude than, and equal duration to the previous example. Under ideal conditions it is very selective and produces essentially the full amplitude in-slice. With a short T_2, its transverse profile is again little changed.

Finally in Fig. 4A we show the transverse profile (not summed) produced by a single excitation using the pulse in Fig. 2A and in Fig. 4B, that produced by a single excitation using the pulse in Fig. 3A. Note that the transverse profile has a very complicated phase relation, which needs to be respected in order to solve the half pulse synthesis problem. This is a reason why an implementation of the inverse scattering transform is needed to solve this type of pulse design problem. The transverse profile for the second pulse shows a much more rapidly decaying imaginary part.

Example 4. Fig. 4C shows the transverse profile produced by a minimum energy 90° pulse with the same bandwidth and transition region as that of the pulses in Examples 2 and 3. It has a duration of 5 ms and requires 2.5 ms of rephasing. For this simulation we set $T_2 = 5$ ms. Comparing this plot to Figs. 1–3C, we see that the transverse profile of the minimum energy pulse suffers much greater loss of amplitude than the summed amplitude produced by the half pulses.

Example 5. For our final example we use a target magnetization with nontrivial real and imaginary parts. The target magnetization, shown in Fig. 5E, has two passbands with the magnetizations 90° out of phase. The pair of half pulses, found using Eq. (15), are shown in Figs. 5A and B. They both have nontrivial real and imaginary parts. The magnetizations produced by each pulse separately are shown in Figs. 5C and D,

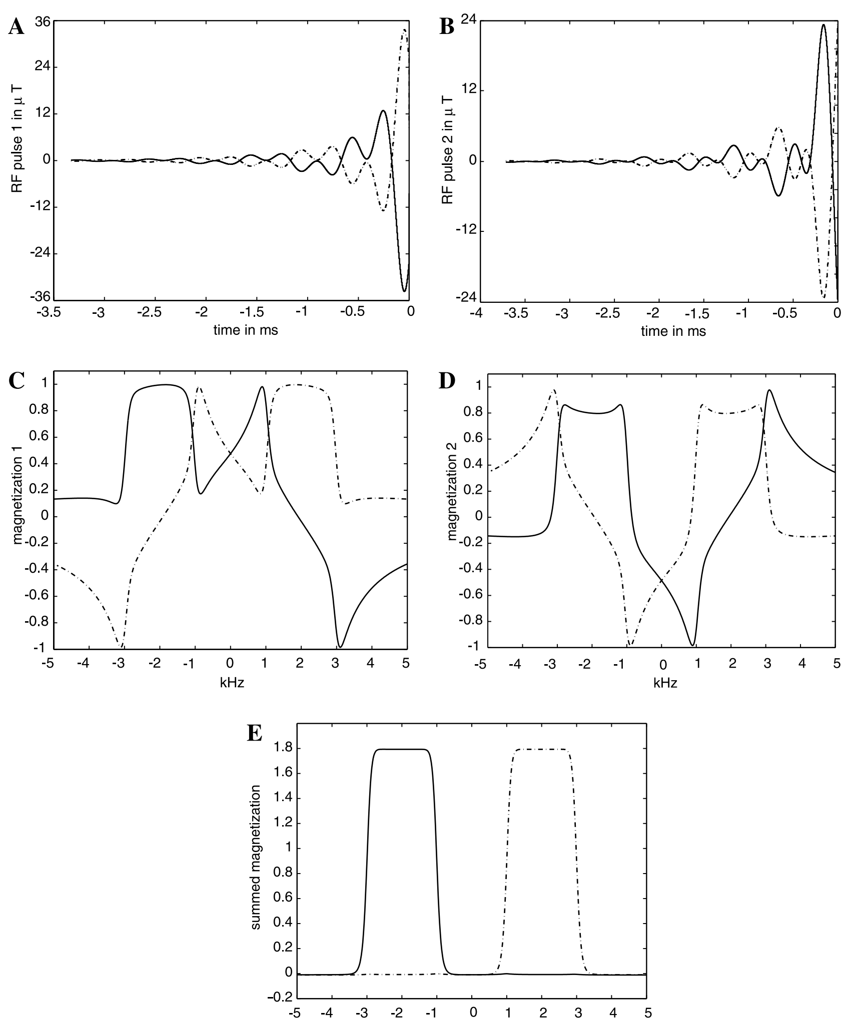

Fig. 5. An example with a nonreal target magnetization. (A) Pulse 1. (B) Pulse 2. (C) The transverse magnetization produced by using the pulse in (A). (D) The transverse magnetization produced by using the pulse in (B). (E) The summed transverse magnetization produced by using the pulses in (A and B). In these plots, the real part is shown as a solid line and the imaginary part as a dot-dash line.

respectively. The summed transverse magnetization is shown in Fig. 5E. This pulse is intended to demonstrate the capabilities of our general algorithm, it is likely far too long to be used in applications where T_2 is very short.

6. Conclusion

We have shown that the problem of half pulse design has a natural interpretation in the inverse scattering formalism introduced in [8,2]. This interpretation leads to simple and efficient algorithms for the exact solution of the general half pulse design problem. In examples, we have seen that, under ideal conditions, the IST designed pulses achieve the specified target summed transverse profile to a very high degree of precision. With a short T_2 the summed profile retains its amplitude and general shape.

In Nielson et al. various practical difficulties with implementing half pulses are discussed. For example, the pulses produced by either the linear or nonlinear theory produce considerable excitation outside the desired slice. The selectivity of the pair of pulses results from delicate cancellations between the out-of-slice contributions from the two excitations. A variety of phenomena, such as eddy currents, can lead to imperfect cancellation out-of-slice, in the sum of the measured signals. To attain a high degree of cancellation, Nielson et al. found it necessary to measure the actual gradient fields, with the sample in place. They then use a VeRSE technique, to match the play out of the half pulses to the actual time course of the gradient. As the VeRSE technique amounts to a change in the time parametrization in Bloch's equations and because the cancellation phenomenon is the result of a symmetry in Bloch's equation, the methods that they employ should work equally well with half pulses designed using the IST approach. With sufficiently good experimental technique, the improvements in the designed profiles should be reflected in the profiles obtained on the scanner.

We have also shown that, by using Blaschke factors with the nonlinear approach, the out-of-slice excitation can be dramatically reduced. As the IST approach gives an infinite dimensional space of solutions to the half pulse synthesis problem, it may be possible to choose the auxiliary parameters to ameliorate the problems that arise in the actual implementation of these pulses.

Acknowledgment

We thank the referees for their careful readings of our paper and their many useful remarks.

Appendix A. Self refocused pulses

If $q(t)$ is supported in $(-\infty, 0]$, then $b(\xi)$ has an analytic extension to the upper half plane and therefore $r(\xi) = b(\xi)/a(\xi)$ has at least a meromorphic extension as well. If $q(t)$ is minimum energy, then $a(\xi)$ is nonvanishing in the upper half plane, and therefore $r(\xi)$ is analytic in the upper half plane as well. On the other hand, if $q(t)$ has minimum energy, then the integrand $f(t)$ for the right Marchenko equation (see Eq. (56) in [2]) is the inverse Fourier transform of $r(\xi)$. If $r(\xi)$ has an analytic extension to the upper half plane, then the Paley–Wiener theorem implies that $f(t)$ has support in the $(-\infty, 0]$. It follows easily from Theorem 3 in [2] that $q(t)$ also has support in $(-\infty, 0]$.

If $r(\xi)$ has a meromorphic extension to the upper half plane with finitely many poles, then, we use the formula for the kernel of the right Marchenko equation as the inverse Fourier transform of $r(\xi + i\eta)$ along a line $\eta =$ constant. It is again a consequence of the Paley–Wiener theorem that $f(t)$ is supported in $(-\infty, 0]$, provided the line of integration lies above all the poles of r. In other words, all of the poles of r in the upper half plane are used to define the data for bound states.

Appendix B. Half pulses with nonreal target transverse profiles

For the general case, we use elementary functional analysis to show that the half pulse synthesis problem has a unique minimum energy solution, for sufficiently small transverse magnetization profiles. We let H_1 denote functions defined on $\mathbb{R}$ such that the function and its first derivative are square integrable. We define a norm on H_1 by setting

$$||f||_1^2 = \int_{-\infty}^{\infty} [|f(\xi)|^2 + |f'(\xi)|^2] \, d\xi.$$

The closed subspace of H_1 consisting of functions with an analytic extension to the upper half plane is denoted by H_1^+. The Paley–Wiener theorem states that a function in H_1 belongs to H_1^+ if and only if its Fourier transform is supported in $(-\infty, 0]$.

Formally the first derivative of the map,

$$S(r_1, r_2) = \frac{2r_1(\xi)}{1 + |r_1(\xi)|^2} + \frac{2r_2(-\xi)}{1 + |r_2(-\xi)|^2}, \tag{B.1}$$

is given by:

$$\delta S(r_1, r_2)[h_1, h_2] = 2\frac{h_1(\xi) - r_1^2(\xi)h_1^*(\xi)}{(1 + |r_1(\xi)|^2)^2} + 2\frac{h_2(-\xi) - r_2^2(-\xi)h_2^*(-\xi)}{(1 + |r_2(-\xi)|^2)^2}. \tag{B.2}$$

The following lemma is not difficult to prove:

Lemma 1. The map $S : H_1^+ \oplus H_1^+ \to H_1$ is bounded and differentiable, with derivative given by Eq. (B.2).

As S is a differentiable map from a Hilbert space to a Hilbert space, we can apply the inverse function theorem to study its invertibility, see [1]. If we can show that $\delta S(0,0)$ is a linear isomorphism from $H_1^+ \oplus H_1^+$ to H_1, then it would follow that the half pulse synthesis problem has a unique small energy solution for small data. Formula Eq. (B.2) gives

$$\delta S(0,0)[h_1,h_2](\xi) = 2(h_1(\xi) + h_2(-\xi)). \tag{B.3}$$

It follows easily from Theorem 1 that $\delta S(0,0)$ is an isomorphism. This proves the following result:

Theorem 2. *If $\mathbf{m}_{xy}^s$ is a function in H_1 with sufficiently small H_1-norm then there is a unique pair of half pulses with small H_1-norm, (q_1, q_2), whose reflection coefficients*, (r_1, r_2), satisfy Eq. (4).

Remark 1. From our experiments it seems likely that much more is true. Indeed one might reasonably hope that, for any function $\mathbf{m}_{xy}^s$ with finite H_1-norm, and maximum modulus less than two, there are pairs of half pulses, which satisfy Eq. (4).

References

[1] M.S. Berger, Nonlinearity and Functional Analysis: Lectures on Nonlinear Problems in Mathematical Analysis, Academic Press, New York, 1977.

[2] C.L. Epstein, Minimum power pulse synthesis via the inverse scattering transform, J. Magn. Reson. 167 (2004) 185–210.

[3] J. Magland, C.L. Epstein, Practical pulse synthesis via the discrete inverse scattering transform, J. Magn. Reson. (2004) 1–26, in press.

[4] H.T. Nielson, G.E. Gold, E.W. Olcott, J.M. Pauly, D.G. Nishimura, Ultra-short echo-time 2D time-of-flight MR angiography using a half-pulse excitation, Magn. Res. Med. 41 (1999) 591–599.

[5] J. Pauly, P. Le Roux, D. Nishimura, A. Macovski, Parameter relations for the Shinnar–Le Roux selective excitation pulse design algorithm, IEEE Trans. Med. Imaging 10 (1991) 53–65.

[6] J. Pauly, D. Nishimura, A. Macovski, A k-space analysis of small-tip-angle excitation, J. Magn. Reson. 81 (1989) 43–56.

[7] M. Robson, P. Gatehouse, G. Bydder, S. Neubauer, Human imaging of phosphorus in cortical and trabecular bone in vivo, Magn. Res. Med. 51 (2004) 888–892.

[8] D.E. Rourke, P.G. Morris, The inverse scattering transform and its use in the exact inversion of the Bloch equation for noninteracting spins, J. Magn. Reson. 99 (1992) 118–138.

[9] A. Yagle, Inversion of the Bloch transform in magnetic resonance imaging using asymmetric two-component inverse scattering, Inverse Problems 6 (1990) 133–151.